Research Square

Preprints are preliminary reports that have not undergone peer review.
They should not be considered conclusive, used to inform clinical practice,
or referenced by the media as validated information.

# Metal Doping Silicates as Inorganic Ion Exchange Materials for Environmental Remediation

**Mamdouh Mohamed Abou-Mesalam**
Egyptian Atomic Energy Authority
**Mohamed Ragab Abass** ( mohamed.ragab2014300@yahoo.com )
Egyptian Atomic Energy Authority https://orcid.org/0000-0002-1766-0449
**Essam Saleh Zakaria**
Egyptian Atomic Energy Authority
**Ali Mostafa Hassan**
Al-Azhar University Faculty of Science

**Research Article**

**Keywords:** In-Situ. Distribution Coefficients. Langmuir Isotherm. Column.

**Posted Date:** August 30th, 2021

**DOI:** https://doi.org/10.21203/rs.3.rs-845617/v1

**License:** This work is licensed under a Creative Commons Attribution 4.0 International License.
Read Full License

**Version of Record:** A version of this preprint was published at Silicon on January 19th, 2022. See the published version at https://doi.org/10.1007/s12633-021-01568-5.

# Metal Doping Silicates as Inorganic Ion Exchange Materials for Environmental Remediation

**Mamdouh M. Abou-Mesalam[a], Mohamed R. Abass[a*], Essam S. Zakaria[a], and Ali M. Hassan[b]**

[a]Egyptian Atomic Energy Authority, Hot Laboratories, and Waste Management Center, 13759, Egypt.

[b]Chemistry Department, Faculty of Science, Al-Azhar University, Cairo, Egypt.

***Corresponding Author:** (M.R. Abass)

E-mail; mohamed.ragab2014300@yahoo.com

Mobile phone: 00201143778444

**E-mail of Authors**

| Name | E-mail | Affiliation | ORCID |
|---|---|---|---|
| Mamdouh M. Abou-Mesalam | mabumesalam@yahoo.com | Egyptian Atomic Energy Authority | |
| Mohamed R. Abass | mohamed.ragab2014300@yahoo.com | Egyptian Atomic Energy Authority | 0000-0002-1766-0449 |
| Essam S. Zakaria | essamzakareya@yahoo.com | Egyptian Atomic Energy Authority | |
| Ali M. Hassan | alimhassanuk@yahoo.co.uk | Faculty of Science, Al-Azhar University, Cairo, Egypt | |


## Highlights

- Titano-silicate and in-situ dopped composites were prepared by precipitation technique.
- The capacity for Co(II), & Cd(II) ions sorbed on Co-TiSi, and Cd-TiSi is higher than obtained for TiSi by 1.81, and 1.41 values, respectively.
- Co-TiSi is suitable for the column technique for the removal of studied cations.

**Abstract**

Titano-silicate (TiSi) and in-situ dopped composites were obtained by precipitation technique. The composition of these materials was established by IR, XRD, TGA&DTA, and XRF. The capacity for Co(II), & Cd(II) ions revealed that Co-TiSi & Cd-TiSi is a higher capacity than those obtained for TiSi by 1.81, & 1.41 values, respectively. To explore the separation potentiality of Co-TiSi for studied cations distribution coefficients in $HNO_3$ were estimated. Langmuir isotherm model is the most representative for discussing the sorption process with a maximum sorption capacity of 16.02, and 10.96 mg/g for Co(II), & Cd(II) ions, respectively. Co-TiSi is suitable for the column technique for the recovery of studied cations. The investigation proved that Co-TiSi composite is suitable for the uptake of the studied ions from liquid solutions and could be considered as potential material for the refining of effluent polluted with these ions.

**Keywords:** In-Situ. Distribution Coefficients. Langmuir Isotherm. Column.

## 1. Introduction

Radwaste is produced through a wide range of operations in power plants, recycling plants, research facilities, and radioisotopes in industry and diagnostic medicine [1]. The stream of waste from nuclear facilities includes low, intermediate, and highly radioactive wastes and may also include a-emitting radioisotopes. In addition to radioisotopes, these streams could contain various toxic and hazardous materials like heavy metals, organic material from decontamination procedures, etc. These wastes must be treated to decrease the radioisotopes concentrations to levels suitable for discharge to the area [1]. Cobalt is one of these metals that is used in nuclear, medical, enamel, and semiconductor industries, grinding wheels, glass, and porcelain painting, hygrometers, and electricity galvanizing. It is also used as a foam stabilizer in beer, in vitamin manufacture, as a drier for lacquers, varnishes, paints. Cobalt can have various adverse effects on health such as asthma, heart damage, heart failure, damage to the thyroid and liver [2]. Cadmium is common for electroplating, nuclear reactors, certain industrial paints, and batteries of nickel-cadmium [3]. Consistent estimation of Cd(II) ion is very important because of its toxic nature. In addition, Cd(II) ion has many radioisotopes along with $^{109}$Cd: it's $t_{0.5}$ of 1.27 years and decays by electron capture to $^{109}$Ag with 88.03 keV emission γ-photons [3] and used as rods for controlling and shielding the absorption of neutrons in reactors with supplementary components [3]. The retention of Co(II) & Cd(II) ions from liquid and radioactive waste solutions was achieved by many researchers [3–8]. Owing to their thermal and radiation tolerance and their opposition to chemical weapons attacks, inorganic ion exchangers now play a significant role in analytical chemistry [9]. Clays and bentonites are naturally occurring materials that have some ion-exchange properties but often it is difficult to use them, for example, in column operation [10]. Synthetic sorbents are used on

an extensive range for different applications, extending from environmental therapy, water softening, hydrometallurgy [11], biochemistry [12], catalysis, and selective adsorption [13–15] to medical applications [16]. Different inorganic sorbents based on silicates were prepared by Abou-Mesalam et al. [17, 18] and utilized for the elimination of some hazardous metals from industrial, environmental, and hazardous wastes. In this article titano-silicate and hazardous doped elements like; Co(II) & Cd(II) ions were synthesized by precipitation method. The materials obtained were established using various analytical tools and exemplified a new sorbent character compared to the original ones. Formulas and applications of obtained compounds for the uptake of some toxic ions from the wastewater solution were done.

## 2. Experimental

### 2.1. Materials

$TiCl_4$ (Merk), $HNO_3$ (Koch-light- Itd Cdnbrook Buks England), $Na_2SiO_3$, $CoCl_2.6H_2O$, & $CdCl_2.4H_2O$ (Alpha Chemika, India), HCl,& $NH_3$ (El-Nasr Co., Egypt). In this analysis, the purity of the chemical used was analytically tested. For all experiments, double distilled water (DDW) was utilized.

### 2.2. Preparation

TiSi composite was fabricated by the dropwise addition of $Na_2SiO_3$ to $TiCl_4$ equimolar solutions (0.05 M) with a volumetric ratio of Ti/Si equal 1.5 at 25±1 °C and constant stirring as a replacement reaction (Scheme 1). Diluted $NH_3$ (10 %) was applied after complete addition before precipitation occurred and then a reaction mixture remained standing overnight. A precipitate was decanted and washed by DDW. In an electric drying oven, the precipitate was dried at 60 $^oC$, grained and sieved for various mesh sizes, and held at 25±1 °C.

Doping of some toxic elements like Co(II) & Cd(II) ions with TiSi composite was synthesized by addition of equimolar solutions (0.05 M) of $Na_2SiO_3$ to $TiCl_4$ and metal chloride, $MCl_2$ with volumetric ratios M:Ti:Si=1:1.5:1 (where M are Co and/or Cd) with agitation at 25±1 $^oC$ as substitution reaction (Scheme 2). With the same method as TiSi, the mixed solutions were immediately hydrolyzed with DDW.

### 2.3. Characterization

The stoichiometry of the constituents in TiSi and metal in-situ doping composites was detected by Philips sequential x-ray spectrometer-2400. The percent of Ti, Si, Co and Cd were measured according to Super-Q quantitative application program. All studied powders were analyzed with IR spectrophotometer (Alpha II Bruker, Germany) at 4000-400 $cm^{-1}$. XRD patterns of prepared powders were take placed using a Shimadzu XD-D1, X-ray diffractometer with Cu-Kα radiation tube source (λ=1.5406 A°), and graphite monochromator working at 30 kV and 30 mA. Prepared powders were

analyzed for DTA & TGA with a sample holder made of Pt in the $N_2$ atmosphere using a Shimadzu DTG-60 H.

### 2.4. Adsorption investigations

#### 2.4.1. Influence of contact time

All the measurement of equilibrium was done by shaking 0.05 g of TiSi sorbent with 2.5 mL of Co(II), and/or Cd(II) ions (50 mg/L) in a shaker thermostat at 25±1 ºC with V/m=50 mL/g. After an interval in time, the shaker is stopped and the solution is isolated at once from the solid. Hence, an atomic absorption spectrometer (AAS) was utilized to detect the concentration of metal ions found in the filtrate. The percent uptake can be computed by equation [15];

$$\% \text{ uptake} = \left( \frac{C_i - C_f}{C_i} \right) 100 \qquad (1)$$

where: $C_i$ & $C_f$, initial & final concentration (mg/L) of Co(II), and/or Cd(II) ions in solution.

#### 2.4.2. Influence of batch factor

A batch factor was optimized to obtain varying V/m ratios (V/m=25, 50, 100, 200, and 400 mL/g) by shaking various weights of composite with different volumes of studied cations. The solutions were separated after equilibrium and the filtrate was taken to test for the metal ion

#### 2.4.3. Capacity measurements

For capacity assessment, regular batch balancing of metal chloride solutions Co(II), and/or Cd(II) ions with the solid materials in the 50 mL/g V/m ratios was performed. A solution was blended at 25±1 °C in such a blender thermostat. The solid was isolated after standing overnight and concentration for ions was determined. From the next equation, a capacity was calculated [19]:

$$\text{Capacity} = \Sigma \text{Uptake x } C_i \text{ x } \frac{V}{m} \quad \text{mg/g} \qquad (2)$$

where V & m are volume of solution, (L) & weight of composite (g).

#### 2.4.4. Sorption studies

Batch equilibration calculated distribution coefficient ($K_d$) of Co(II), and/or Cd(II) ions on the CoTiSi sorbent. A shaker thermostat fixed at 25±1 °C for 30 minutes was put in the mixture. The solutions were isolated after equilibrium by centrifugation. $K_d$ & separation factor were computed using the following equations [20]:

$$K_d \text{ (mL/g)} = \left( \frac{C_i - C_f}{C_f} \right) \frac{V}{m} \qquad (3)$$

$$\text{Separation factor } (\alpha^a{}_b) = \frac{K_d(b)}{K_d(a)} \quad (4)$$

where; $K_d$ (a) & $K_d$ (b) are distribution coefficients for the two conflicting species a & b in the system.

### 2.4.5. Sorption isotherm

Sorption isotherms of studied cations on CoTiSi sorbent were determined over the entire concentration range (100-1000 mg/L) at a constant V/m ratio of 50 mL/g. The testing was achieved in a shaker thermostat at 25±1 ˚C. An equilibrium concentration ($C_{eq}$) and amount uptake ($q_e$) were calculated in mg/g as follows [20];

$$q_e\,(mg/g) = \frac{uptake.C_i.V}{m} \qquad (5)$$

$$C_{eq} = C_i\left(\frac{(1-uptake)}{100}\right) \qquad (6)$$

A plot of $\log C_{eq}$ against $\log q_e$ and/or $C_{eq}$ against $C_{eq}/q_e$ was achieved to reach the applicable isotherm model.

### 2.4.6. Column investigations

Chromatographic columns breakthrough investigations were conducted as follows, 0.5 g of CoTiSi with particle size 0.380 mm were packed in a glass column (0.6 cm diameter and 5 cm heights) to give a bed height of 1.1 $cm^3$ volume. 1000 mL of the desired solutions (pH = 3) containing 50 mL/g of metal chloride of studied cations were passed through the column beds at a flow rate of four drops/min, equal portions were collected and the concentrations were continuously measured. The values of breakthrough capacity were calculated using the formula [15];

$$\text{Breakthrough capacity}\,(mg/g) = \frac{V_{(50\%)}.C_i}{m} \qquad (7)$$

where; $V_{(50\%)}$ is a volume for effluent at 50 percent breakthrough (L).

Distilled water and different $NaNO_3$ concentrations (0.01-0.5 M) were used to elute Co(II), and/or Cd(II) ions loaded CoTiSi composite at the flow rate of 4 drops/min, the eluent was collected every 20 min and the concentrations were measured.

## 3. Results & Discussion

The focus of this paper is to synthesize highly selective ion-exchangers in certain toxic metals. For the four ion exchangers, TiSi and its in situ dopant composites CoTiSi, and CdTiSi were fabricated with comprehensive characterization.

### 3.1. Characterization

IR spectra (Fig. 1A), reveal that five characteristic bands were observed in regions 2800-3500, 1625, 1335, 1000, and 800-480 $cm^{-1}$ for each TiSi, CoTiSi, and CdTiSi composite. The absorption band

found at 2820-3500 $cm^{-1}$ for these substances can be due to the free water and OH groups absorbed by the composites in stretching mode [15, 19]. In-situ doping of Co(II), and/or Cd(II) ions with TiSi composites reduces the strength of this band. This decrease may be related to the reduction of the $H_2O$ content of metals by in-situ doping. At 1625 $cm^{-1}$, a strong band attributed to a bending vibration for water molecules absorbed on composites prepared [21, 22]. At 1000 $cm^{-1}$ due to Ti-OH deformation vibration [23], or overlapping of the Si-O and Si-OH [20], and Ti-O bonds in the structure, the band appeared at 780 $cm^{-1}$ [24]. Two bands at 567 and 480 $cm^{-1}$ are assigned to Si-O-Ti and Si-O-Si (bending vibrations), respectively [24]. Bands at 416-465 $cm^{-1}$ are associated with metal-O bonds (Co, Cd-O) [21].

XRD of prepared composites (Fig. 1B), reveals that TiSi and in-situ doping composites have a crystalline structure. A crystallinity of TiSi was increased with in-situ Cd(II) ion and reduced with in-situ Co(II) ion with TiSi. This variation may be related to the role of a radius of in-situ ions, where a radius of Co(II) ion is smaller than Cd(II) ion. This means that the ions hold with the $H_2O$ in the surface of the composite according to unhydrated order Co(II)>Cd(II) and leads to an increase in the $H_2O$ content and increasing of amorphous nature. These results were agreeing with data obtained from the XRD of composites materials treated at different heating temperatures [25].

Differential thermal & thermogravimetric analyses (DTA&TGA) of studied composites (Fig. 2). In the DTA curve for TiSi, CoTiSi, and CdTiSi one endothermic peaks appear at (108 $^oC$, 104$^oC$, and 94.9 $^oC$) respectively, which may be due to loss in free water [20, 26]. One exothermic peak is appeared at (478$^oC$ & 561$^oC$) for TiSi & CoTiSi respectively, related to the phase change to metal oxide [19, 20]. Due to a loss of chemical bond water, an endothermic peak occurs at 320 $^oC$ for Cd-TiSi [20].
The chemical formula of prepared composites is based on XRF and DTA&TGA whose mass loss allowed the expression to measure a percent of moisture with matrix [20].

$$18n = \frac{x\left(M + 18n\right)}{100} \qquad (8)$$

where X is the percent mass loss of the water, n is the mole number of water and M is the molar weight of a compound without water molecules. An X value was found 15.6, 19.6 & 10.8 % for TiSi, CoTiSi & CdTiSi, respectively. The molecular formulas of TiSi & in-situ doping composites were calculated and tabulated within Table 1.

### 3.2. Adsorption investigations

#### 3.2.1. Influence of shaking time

Retention of Co(II), and/or Cd(II) ions onto TiSi with shaking time (Fig. 3A) was done. It is appreciated that % uptake improves with the increasing of agitating time and maximum removal was

detected at 25 min for Cd(II) ion and 30 min for Co(II) ion on TiSi. Therefore, we can consider these times are sufficient to achieve equilibrium for studied cations and used for all further experiments.

### 3.2.2. Batch factor impact (V/m)

The influence of V/m on % uptake of studied cations onto the TiSi (Fig. 3B) was investigated using V/m ratios from 25 to 400 mL/g. The data perfect that % uptake of studied cations on the TiSi decrease with increasing the V/m ratio and the best ratio at V/m 50 mL/g and this ratio was used for further experiments.

### 3.2.3. Capacity measurements

The capacity of TiSi for Co(II), and/or Cd(II) ions was determined at 25±1 ºC (Table 2). Table 2, indicated that the affinity order for all cations is Co(II)>Cd(II), this sequence is in agreement with the unhydrated radii of the exchanging ions. Ions with smaller unhydrated radii simply enter cavities of an exchanger, resulting in higher adsorption [9, 15]. A high TiSi capacity for Co(II) ions also can be due to the greater complexing capacity of cobalt with more than one oxidation state presence [9]. Also, data in Table 2, showed that a capacity of CoTiSi & CdTiSi composites for studied cations is higher than obtained for TiSi by 1.81 & 1.41 values, respectively, with a sequence order; Co(II)>Cd(II) for CoTiSi & CdTiSi. These data imply that by holding the hole for exchangeable ions in a coordination bonding system, a composite can be constructed. A product will display high selectivity for exchangeable ions just as to be kept in ion memory after replacing a particular ion with another ion to maintain fundamentally original structures by impregnation of these cations with TiSi. And the capacity of these composites for Co(II), and/or Cd(II) ions have the sequence order; CoTiSi>CdTiSi>TiSi, so CoTiSi was used for further experiments. Comparable findings were obtained for MgAlSi and MgSi by Abou-Mesalam et al [25]. Comparing these findings with the potential indicated by MgSi and metal in-situ (Co & Cd) for these metals, TiSi has a greater capacity than MgSi [20]. A capacities of MgSi, P(AM-AA), and {P(AM-AA)-MgSi} for Ni(II), Cd(II), Co(II), Pb(II), Zn(II) & Cu(II) ions have sequence order: {Cu(II)>Ni(II)≈Co(II)>Pb(II)≥ Zn(II)>Cd(II)}, {Co(II)≥Ni(II)>Pb(II)>Zn(II)>Cd(II)>Cu(II)}, {Co(II)≥Ni(II)>Cu(II)>Zn(II)>Pb(II)>Cd(II)} for MgSi, P(AM-AA) & {P(AM-AA)-MgSi} respectively [9].

### 3.2.4. Influence of $[H^+]$ ion on $K_d$

A separation potentiality of CoTiSi for Co(II), and/or Cd(II) ions can be explored by studying $K_d$ & $\alpha^a{}_b$ at range ($10^{-3}$ - 1 M) $HNO_3$ medium were calculated and tabulated in Table 3. Table 3, indicated that distribution coefficients have an affinity sequence; Co(II)>Cd(II), this sequence supports the sorption of ions in a dehydrated state. $\alpha^a{}_b$ for studied cations were calculated and revealed that Co(II) has a greater separation factor. Table 3, displays the contrariwise proportionality of the removal

213 percentage with the [$H^+$]. Ion mobility of studied cations is decreased by increasing [$H^+$]. A reduction
214 of ion mobilities may be clarified by a growth of the frictional forces exerted in ions because of a
215 change of the nature of hydrogen bonds in water [27]. A subsequent water cluster ions are produced
216 when a proton concentration rises, $H_3O^+$, $H_5O_2^+$, $H_7O_3^+$, $H_9O_4^+$ changing water structure, and thus an
217 ion-water interaction [28]. Also, a sorbent takes $H^+$ from a solution, hence, a surface converts
218 positively charged, which eventually limits the uptake of Co(II), and/or Cd(II) ions [27].

219 **3.2.5. Sorption isotherm**

220 The nature of adsorption processes for studied cations on CoTiSi was investigated by a steady rise of
221 the sorbate concentration and determining the quantity sorbed at each equilibrium concentration. Two
222 types of isothermal equations were conventional for the sorption data (Freundlich & Langmuir).
223 Freundlich isotherm used mathematical model extensively, given a heterogeneous surface expression
224 observed and a probability function of functional groups and their energies measured in the next
225 equation [20]:

226 $$\log q_e = \log k_F + \frac{1}{n}\log C_{eq} \qquad (9)$$

227 where $K_F$ &1/n are Freundlich constants integrating all aspects disturbing adsorption procedure such
228 as adsorption intensity and capacity of adsorption and computed from both slope & intercept of a linear
229 plot of $\log q_e$ & $\log C_{eq}$, as exposed in Fig. 4A. Higher $K_F$ values show greater Co(II), & Cd(II) ions
230 affinity. Adsorption intensity or heterogeneity for a surface is calculated through slope 1/n [20]. $K_F$,
231 $R^2$ & $n^{-1}$ are existing in Table 4. As exposed in Table 4, $n^{-1}<1$ values show promising ion exchangers
232 [29].

233 The adsorption model Langmuir adsorbs molecules in a fixed set of well-defined locations, each of
234 which has a single molecule and no adsorbate movement at the surface level. These positions are
235 therefore energy equal and distant, so there are no interactions between adsorbed molecules in their
236 neighboring locations. By the next equation [29], a linear form of Langmuir is determined:

237 $$\frac{C_{eq}}{q_e} = \frac{C_{eq}}{q_m} + \frac{1}{K_L q_m} \qquad (10)$$

238 In which $q_m$ & $K_L$ are Langmuir constants involving adsorption capacity & energy of adsorption and
239 computed from slope & intercept respectively for plots of $C_{eq}/q_e$ & $C_{eq}$. The linearized Langmuir
240 adsorption of Co(II), & Cd(II) ions at (Fig. 4B). Constants ($q_m$ & $K_L$) assessed from isotherms and
241 their $R^2$ are existing in Table 4, and this data, reveals that Freundlich isotherm provides fit to
242 equilibrium adsorption data, giving $R^2$ of Co(II), & Cd(II) ions (0.986, and 0.949), while Langmuir

isotherm provides a brilliant fit to equilibrium adsorption data, giving $R^2$ of Co(II), & Cd(II) ions (0.988, and 0.9995). From these data, the Langmuir is more relevant than the Freundlich model.

### 3.2.6. Column operations

Fig. 5A shows the breakthrough curves for studied cations (50 mg/L for each) onto the CoTiSi column, which depicts % concentrations of a respective metal ion within an effluent to a feed solution ($C/C_o$ %) Vs. effluent volume (mL), a corresponding uptake of Co(II), & Cd(II) ions per gram for solid is calculated from Fig. 5A using equation (7). A breakthrough capacity for all ions studied is calculated from Fig. 4B and found to be 26.0, and 17.0 mg/g for Co(II), & Cd(II) ions respectively. From these results, it is found that selectivity followed order: Co(II)>Cd(II). This sequence supported that the sorption process was taking place in dehydrated ionic radii, ions with smaller dehydrated ionic radii easily enter cavities of an exchanger resulting in a higher uptake [9]. And a column technique breakthrough capacity is smaller than the capacity measured from a batch technique. These results reflect a great competition of ions sorbed. From these data, it can be assumed that: CoTiSi sorbent is suitable for the sorption of Co(II), & Cd(II) ions from aqueous elutions at pH = 3.

### 3.2.7. Elution studies

The elution profile for Co(II), & Cd(II) ions is illustrated in Figure 5B. The elution of the investigated ions is studied using DDW and different $NaNO_3$ concentrations (0.01, 0.05, 0.1, and 0.5 M). Cd(II) ions were released using 0.01 M $NaNO_3$ as eluent. However, the separation of Co(II) ions was released using 0.05, and 0.1 M $NaNO_3$ as eluent. At 0.5 M $NaNO_3$, the column packed with CoTiSi becomes free from any sorbed metal ions and can be reused again for chromatographic separation. From these data Cd(II) ion can be separated from Co(II) ion using 0.01 M $NaNO_3$ as eluent.

## 4. Conclusion

Titano-silicate and in-situ dopant composites were synthesized, characterized, and employed for batch sorption of cobalt & cadmium ions from an aqueous medium in this study. Titano-silicate and in-situ dopant composites with formulas $Ti_{4.2}Si_{0.2}O.2.2H_2O$, $Co_{2.3}Ti_{20.8}SiO_{0.17}.15.8H_2O$ & $Cd_{0.16}Ti_{22.3}SiO_{9.2}.8.5H_2O$, respectively were produced by precipitation technique. The capacity reveals that prepared composites have high values comparing with inorganic sorbents and CoTiSi is the best sample. The distribution coefficients at different concentrations of hydrogen ion have selectivity order: Co(II)>Cd(II). Langmuir isotherm is more applicable isotherms. Finally, TiSi is suitable for a column technique. Finally, from the chromatographic column, CoTiSi can be working as an active sorbent to separate Cd(II) ion from Co(II) ion using 0.01 M $NaNO_3$ as eluent.

**Funding information**

Not applicable

**Conflicts of Interest**

The authors whose names are listed immediately below certify that they have NO affiliations with or involvement in any organization or entity with any financial interest (such as honoraria; educational grants; participation in speakers' bureaus; membership, employment, consultancies, stock ownership, or other equity interest; and expert testimony or patent-licensing arrangements), or non-financial interest (such as personal or professional relationships, affiliations, knowledge or beliefs) in the subject matter or materials discussed in this manuscript.

Mamdouh M. Abou-Mesalam, Mohamed R. Abass, Essam S. Zakaria, and Ali M. Hassan

**Author contribution**

**M.R. Abass**: Data curation, writing - original draft review & editing. **E.S. Zakaria, and A.M. Hassan**: Data collection & editing. **M.M. Abou-Mesalam**: review & editing.

**Availability of data and material**

Yes

**Compliance with ethical standards**

Yes

**Consent to participate**

Yes

**Consent for publication**

Yes

**Acknowledgments**

This work has been supported by the Egyptian Atomic Energy Authority and Faculty of Science, Al-Azhar University, Cairo, Egypt. Great thanks to all members of the nuclear fuel technology department, Egyptian Atomic Energy Authority for supporting this work.

## References


1. Nilchi A, Atashi H, Javid AH, Saberi R (2007) Preparations of PAN-based adsorbers for separation of cesium and cobalt from radioactive wastes. Applied Radiation and Isotopes 65:482–487. https://doi.org/10.1016/j.apradiso.2006.12.003
2. Kulkarni SJ (2016) Research and Studies on Cobalt Removal from Wastewater. International Journal of Research and Review 2237:41–44
3. Aglan RF, Hamed MM, Saleh HM (2019) Selective and sensitive determination of Cd (II) ions in various samples using a novel modified carbon paste electrode. Journal of Analytical Science and Technology 10:1–11
4. Dubey A, Mishra A, Singhal S (2014) Application of dried plant biomass as novel low-cost adsorbent for removal of cadmium from aqueous solution. International journal of environmental science and technology 11:1043–1050
5. Wang FY, Wang H, Ma JW (2010) Adsorption of cadmium(II) ions from aqueous solution by a new low-cost adsorbent-Bamboo charcoal. Journal of hazardous materials 177:300–306
6. Pyrzynska K (2019) Removal of cadmium from wastewaters with low-cost adsorbents. Journal of Environmental Chemical Engineering 7:102795
7. Kang R, Qiu L, Fang L, et al (2016) A novel magnetic and hydrophilic ion-imprinted polymer as a selective sorbent for the removal of cobalt ions from industrial wastewater. Journal of environmental chemical engineering 4:2268–2277
8. Park Y, Lee YC, Shin WS, Choi SJ (2010) Removal of cobalt, strontium, and cesium from radioactive laundry wastewater by ammonium molybdophosphate-polyacrylonitrile (AMP-PAN). Chemical Engineering Journal 162:685–695. https://doi.org/10.1016/j.cej.2010.06.026
9. Abou-Mesalam MM, Abass MR, Abdel-Wahab MA, et al (2018) Polymeric composite materials based on silicate: II. sorption and distribution studies of some hazardous metals on irradiated doped polyacrylamide acrylic acid. Desalination and Water Treatment 109:176–187. https://doi.org/10.5004/dwt.2018.22084
10. De León MA, Sergio M, Bussi J, et al (2019) Heterogeneous photo-Fenton process using iron-modified regional clays as catalysts: photonic and quantum efficiencies. Environmental Science and Pollution Research 26:12720–12730
11. Abou-Mesalam MM, Hilal MA, Arida HA (2013) Environmental studies on the use of synthesized and natural ion exchange materials in the treatment of drinking and underground water. Arab Journal of Nuclear Science and Applications 46:63–74
12. Ali IM, Zakaria ES, Ibrahim MM, El-Naggar IM (2008) Synthesis, structure, dehydration transformations and ion exchange characteristics of iron-silicate with various Si and Fe contents

as mixed oxides. Polyhedron 27:429–439

13. Jin R, Liu Y, Liu G, et al (2020) Influence of chromate adsorption and reduction on transport and retention of biochar colloids in saturated porous media. Colloids and Surfaces A: Physicochemical and Engineering Aspects 124791

14. Yang X, Gu W, Ma Y, et al (2020) Interface electron transfer of $Bi_2MoO_6$/MIL-125 and the visible-light performance for pollutant degradation. Colloids and Surfaces A: Physicochemical and Engineering Aspects 124748

15. Abass MR, El-Masry EH, Ibrahim AB (2021) Preparation, characterization, and applications of polyacrylonitrile/ball clay nanocomposite synthesized by gamma radiation. Environmental Geochemistry and Health 43:3169–3188. https://doi.org/https://doi.org/10.1007/s10653-021-00813-5

16. Lee S, Kim J, Ku B-C, et al (2012) Structural Evolution of Polyacrylonitrile Fibers in Stabilization and Carbonization. Advances in Chemical Engineering and Science 02:275–282. https://doi.org/10.4236/aces.2012.22032

17. Abou-Mesalam MM, Abass MR, Ibrahim AB, Zakaria ES (2020) Polymeric composite materials based on silicate. III-Capacity and sorption behavior of some hazardous metals on irradiated doped polyacrylamide acrylonitrile. Desalination and Water Treatment 193:402–413. https://doi.org/10.5004/dwt.2020.25816

18. Abass MM, Ibrahim AB, El-Masry EH, Abou-Mesalam MM (2021) Optical properties enhancement for polyacrylonitrile-ball clay nanocomposite by heavy metals saturation technique. Journal of Radioanalytical and Nuclear Chemistry 329:849–855. https://doi.org/https://doi.org/10.1007/s10967-021-07844-3

19. Abass MR, Ibrahim AB, Abou-Mesalam MM (2021) Retention and selectivity behavior of some lanthanides using bentonite dolomite as a natural material. Chemical Papers 75:3751–3759. https://doi.org/https://doi.org/10.1007/s11696-021-01621-y

20. Abou-Mesalam MM, Abass MR, Abdel-Wahab MA, et al (2016) Complex doping of d-block elements cobalt, nickel, and cadmium in magneso-silicate composite and its use in the treatment of aqueous waste. Desalination and Water Treatment 57:25757–25764. https://doi.org/10.1080/19443994.2016.1156031

21. Abass MR, Diab HM, Abou-Mesalam MM (2021) New Improved Thermoluminescence Magnesium Silicate Material for Clinical Dosimetry. Silicon 1–9. https://doi.org/https://doi.org/10.1007/s12633-021-01049-9

22. Abou-Mesalam MM, Abass MR, Ibrahim AB, et al (2019) Tunable optical and dielectric properties of polymeric composite materials based on magneso-silicate. Bulletin of Materials

Science 42:31. https://doi.org/https://doi.org/10.1007/s12034-018-1721-0

23. Al-Degs YS, El-Barghouthi MI, Issa AA, et al (2006) Sorption of Zn(II), Pb(II), and Co(II) using natural sorbents: equilibrium and kinetic studies. Water research 40:2645–2658

24. Abou-Mesalam MM, El-Naggar IM (2003) Diffusion mechanism of $Cs^{+}$, $Zn^{2+}$ and $Eu^{3+}$ ions in the particles of zirconium titanate ion exchanger using radioactive tracers. Colloids and Surfaces A: Physicochemical and Engineering Aspects 215: https://doi.org/10.1016/S0927-7757(02)00443-0

25. Abou-Mesalam MM, El-Naggar IM (2008) Selectivity modification by ion memory of magneso-silicate and magnesium alumino-silicate as inorganic sorbents. Journal of Hazardous Materials 154:168–174. https://doi.org/10.1016/j.jhazmat.2007.10.007

26. Andrunik M, Bajda T (2019) Modification of Bentonite with Cationic and Nonionic Surfactants: Structural and Textural Features. Materials 12:3772

27. Moloukhia H (2010) Use of animal charcoal prepared from the bivalve chaelatura (chaelatura) companyoi in treatment of waste solution containing cesium and strontium ions. Journal of Radiation Research and Applied Sciences 3:343–356

28. El-Aryan YF, Abdel-Galil EA, El-deen GES (2015) Synthesis, characterization and adsorption behavior of cesium, cobalt, and europium on organic-inorganic hybrid exchanger. Russian Journal of Applied Chemistry 88:516–523

29. Abdel-Galil EA, Ibrahim AB, Abou-Mesalam MM (2016) Sorption behavior of some lanthanides on polyacrylamide stannic molybdophosphate as organic-inorganic composite. International Journal of Industrial Chemistry 7:231–240

**Table captions:**

**Table 1** Ratio of main elements obtained from XRF and proposed molecular formulas for TiSi and in-situ doping composites.

**Table 2** Capacities of TiSi and in-situ doping composites for Co(II), and Cd(II) ions at 25±1 ˚C.

**Table 3** $K_d$ values & separation factors of Co(II), and Cd(II) ions as a function of $[H^+]$ on CoTiSi.

**Table 4** Freundlich and Langmuir parameters for adsorption of Co(II), and Cd(II) ions onto CoTiSi at at 25±1 ˚C.

435 **Table 1**

| Composites | Ti | Si | Co | Cd | O | $H_2O$ | Molecular formula |
|---|---|---|---|---|---|---|---|
| TiSi | 72.5 | 2.3 | --- | --- | 5.7 | 15.6 | $Ti_{4.2}Si_{0.2}O \cdot 2.2H_2O$ |
| CoTiSi | 63.9 | 1.9 | 8.7 | --- | 0.18 | 19.6 | $Co_{2.3}Ti_{20.8}SiO_{0.17} \cdot 15.8H_2O$ |
| CdTiSi | 68.4 | 1.8 | --- | 1.2 | 9.5 | 10.8 | $Cd_{0.16}Ti_{22.3}SiO_{9.2} \cdot 8.5H_2O$ |

436

437 **Table 2**

| Composites | Water content | Co(II) | | Cd(II) | |
|---|---|---|---|---|---|
| | | Capacity mg/g | Exchanging as | Capacity mg/g | Exchanging as |
| TiSi | %25 | 30.6 | Unhydrated | 8.4 | Unhydrated |
| CoTiSi | %29.5 | 46.4 | Unhydrated | 24.5 | Unhydrated |
| CdTiSi | %29.1 | 34.1 | Unhydrated | 21.2 | Unhydrated |

438

439 **Table 3**

| $[H^+]$ | $K_d$ (mL/g) and (α) | Cd(II) | Co(II) |
|---|---|---|---|
| 0.001 | $K_d$<br>$\alpha^a{}_b$ | 413.0 | 24950.0<br>60.4 |
| 0.01 | $K_d$<br>$\alpha^a{}_b$ | 94.9 | 538.2<br>5.7 |
| 0.1 | $K_d$<br>$\alpha^a{}_b$ | 25.1 | 206.4<br>8.2 |
| 0.5 | $K_d$<br>$\alpha^a{}_b$ | 11.3 | 41.7<br>3.7 |
| 1 | $K_d$<br>$\alpha^a{}_b$ | 5.1 | 20.9<br>4.1 |

440

441 **Table 4**

| Metal ions | Freundlich parameters | | | Langmuir parameters | | | |
|---|---|---|---|---|---|---|---|
| | Adsorption capacity (1/n) | Adsorption intensity $K_F$ | $R^2$ | Adsorption capacity ($q_m$) (mg/g) | Energy of adsorption ($K_L$) (L/g) | Adsorption intensity $R_L$ | $R^2$ |
| Co(II) | 0.124 | 6.328 | 0.986 | 16.015 | 0.029 | 0.087 | 0.988 |
| Cd(II) | 0.310 | 1.381 | 0.949 | 10.963 | 0.012 | 0.181 | 0.995 |

442

443

444

445

446

447

448

**Figure & scheme captions:**

**Scheme 1.** The formation mechanism of TiSi composite.

**Scheme 2.** The formation mechanism of in-situ doping TiSi composites.

**Fig. 1. (A)** IR spectra and **(B)** XRD patterns for TiSi and in-situ doping composites.

**Fig. 2. (A)** TGA and **(B)** DTA for TiSi and in-situ doping composites.

**Fig. 3. (A)** Effect of contact time on % uptake and **(B)** Effect of V/m on % uptake of Co(II), and Cd(II) ions on the TiSi at 25±1$^{o}$C.

**Fig. 4.** Adsorption of Co(II), and Cd(II) ions on the CoTiSi at 25±1$^{o}$C **(A)** Freundlich adsorption isotherm and **(B)** Langmuir adsorption isotherm.

**Fig. 5. (A)** Breakthrough capacity of Co(II), and Cd(II) ions on the CoTiSi at 25±1$^{o}$C and pH 3 **(B)** Chromatographic separation of Co(II), and Cd(II) ions using different eluents.

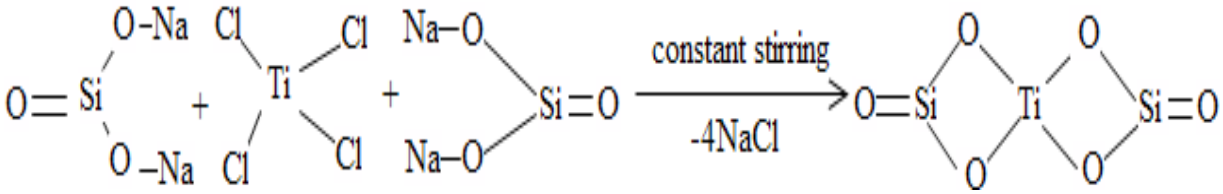


**Scheme 1.**

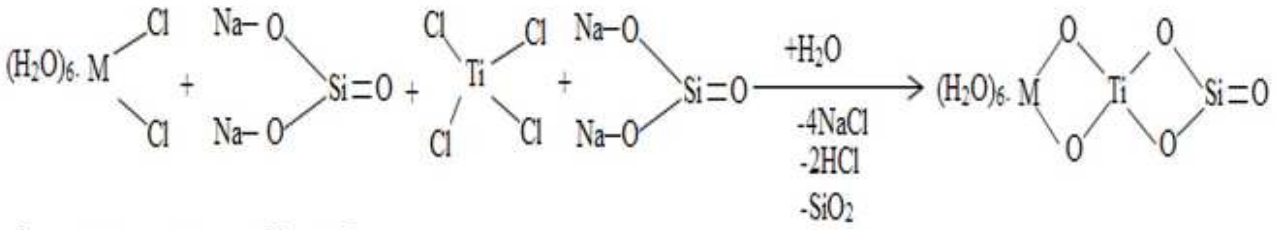


where M are Co and/or Cd

**Scheme 2.**

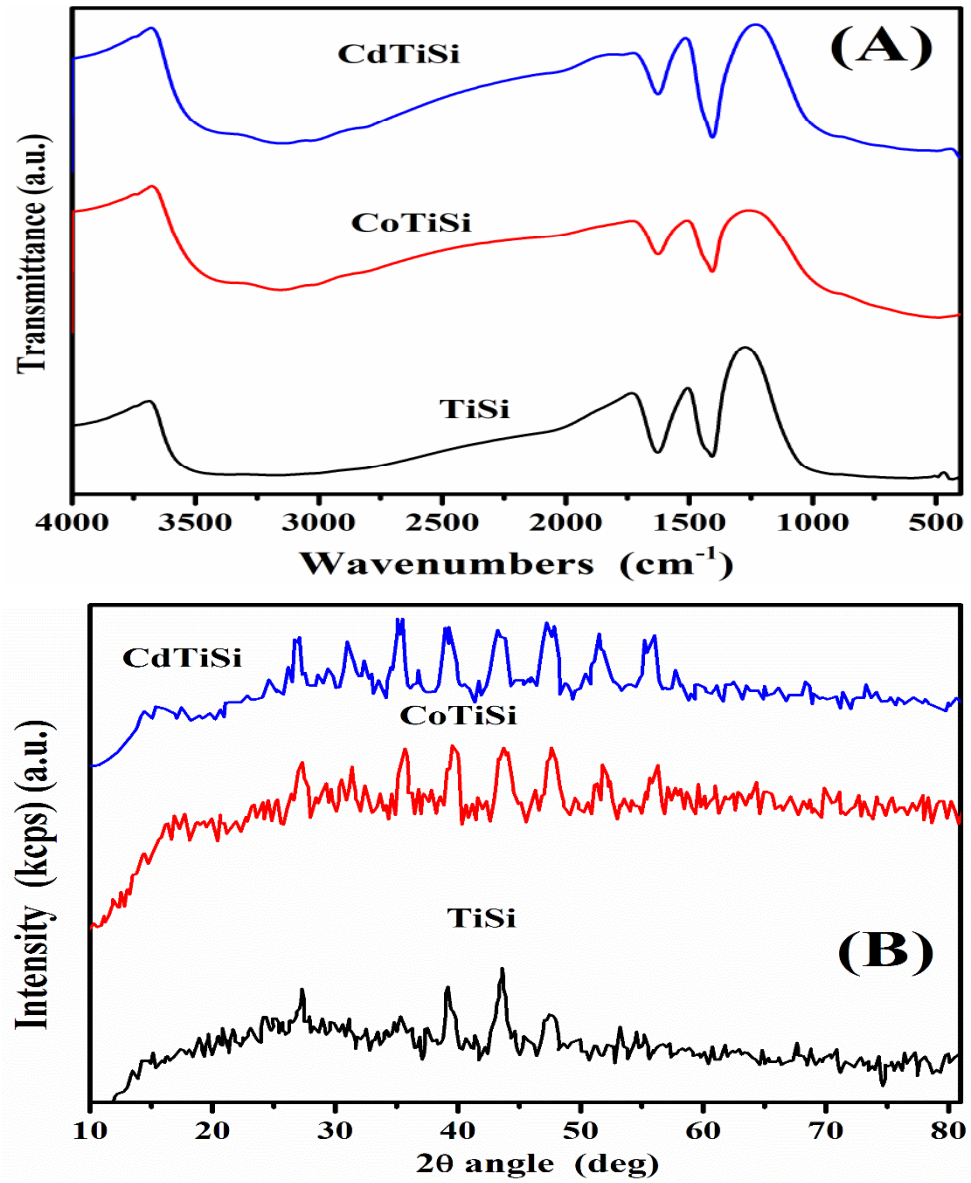
CdTiSi
(A)
CoTiSi
TiSi
Transmittance (a.u.)
4000
3500
3000
2500
2000
1500
1000
500
Wavenumbers (cm-1)
CdTiSi
CoTiSi
TiSi
(B)
Intensity (kcps) (a.u.)
10
20
30
40
50
60
70
80
2θ angle (deg)

**Fig. 1.**

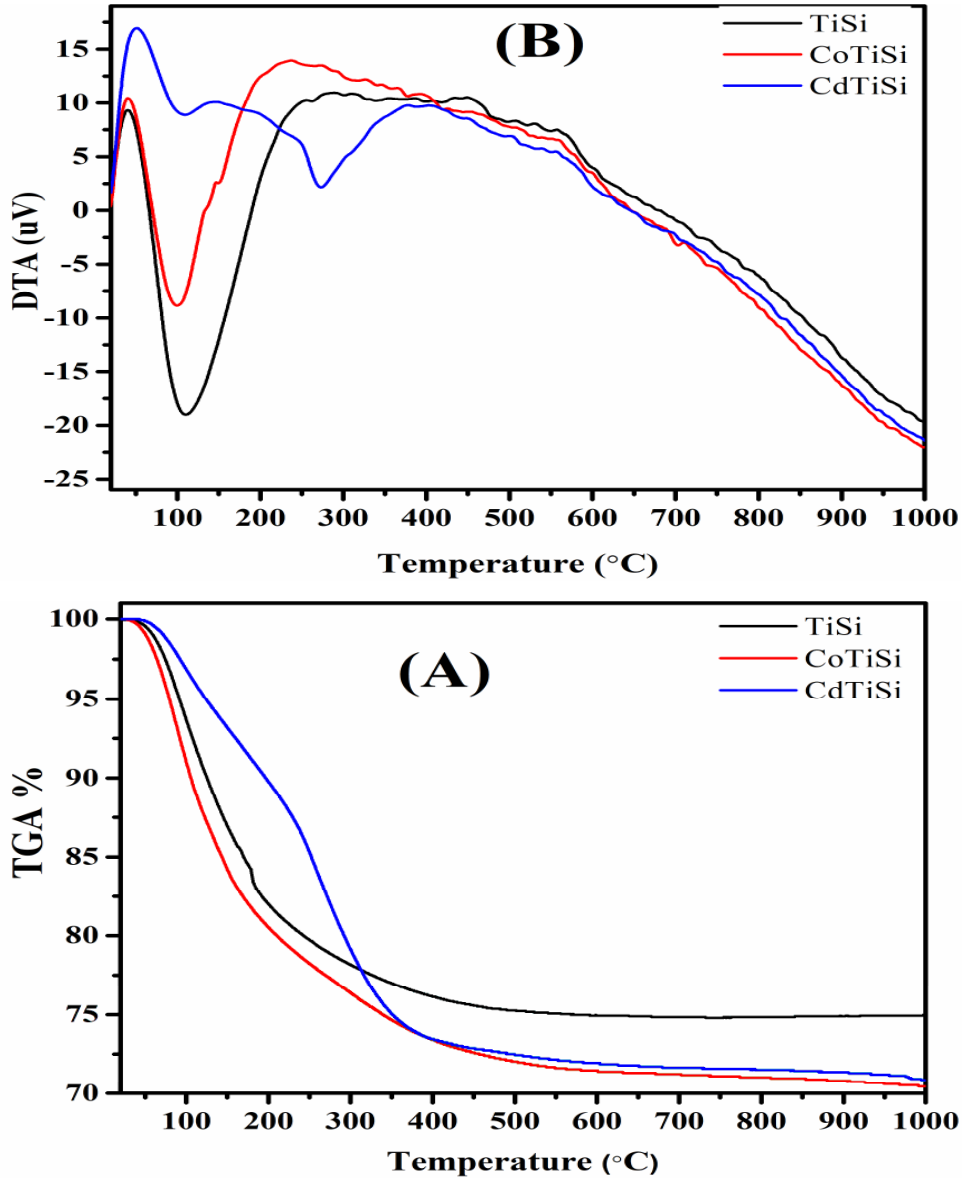
(B)
TiSi
CoTiSi
CdTiSi
DTA (uV)
15
10
5
0
-5
-10
-15
-20
-25
100
200
300
400
500
600
700
800
900
1000
Temperature (°C)
(A)
TiSi
CoTiSi
CdTiSi
TGA %
100
95
90
85
80
75
70
100
200
300
400
500
600
700
800
900
1000
Temperature (°C)

**Fig. 2.**

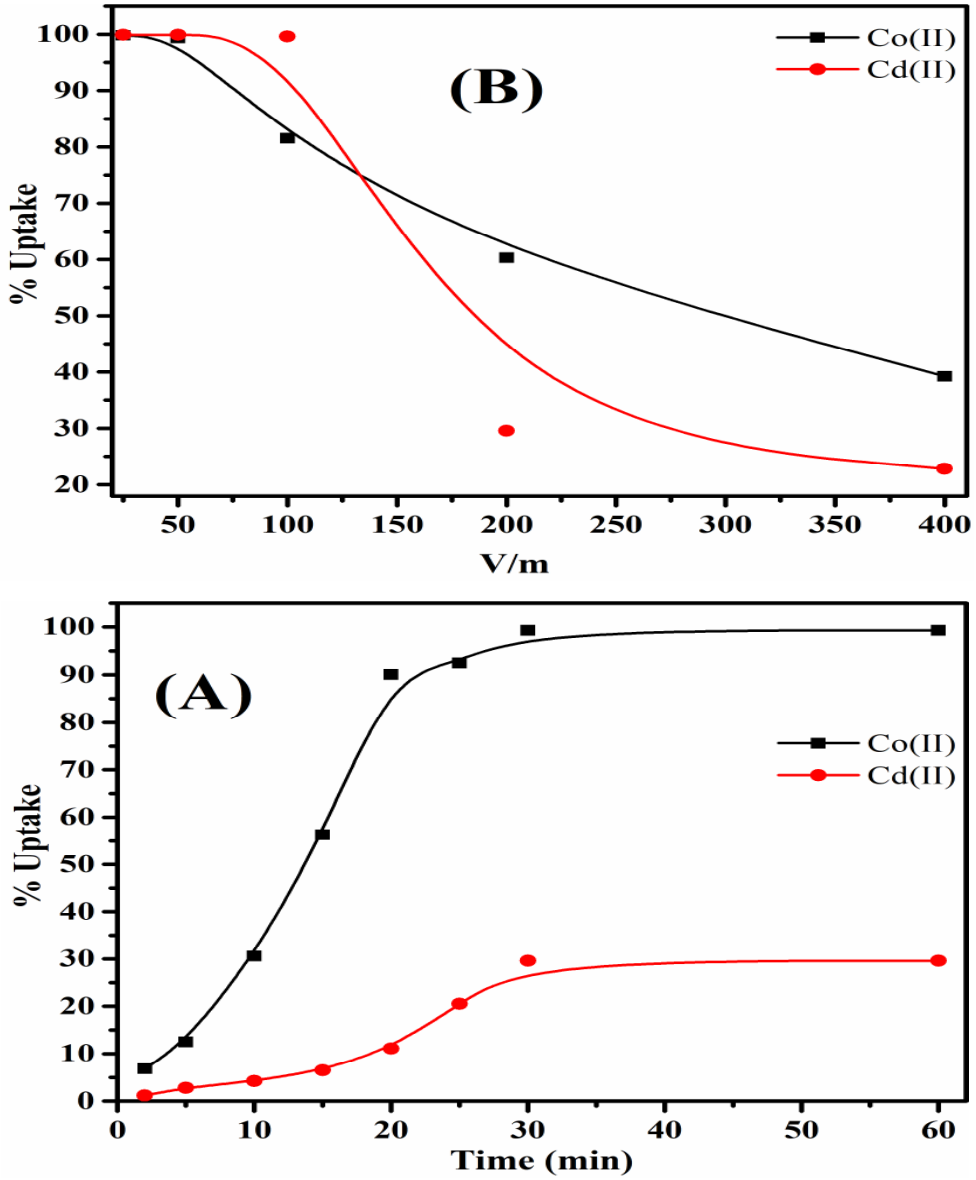


**Fig. 3.**

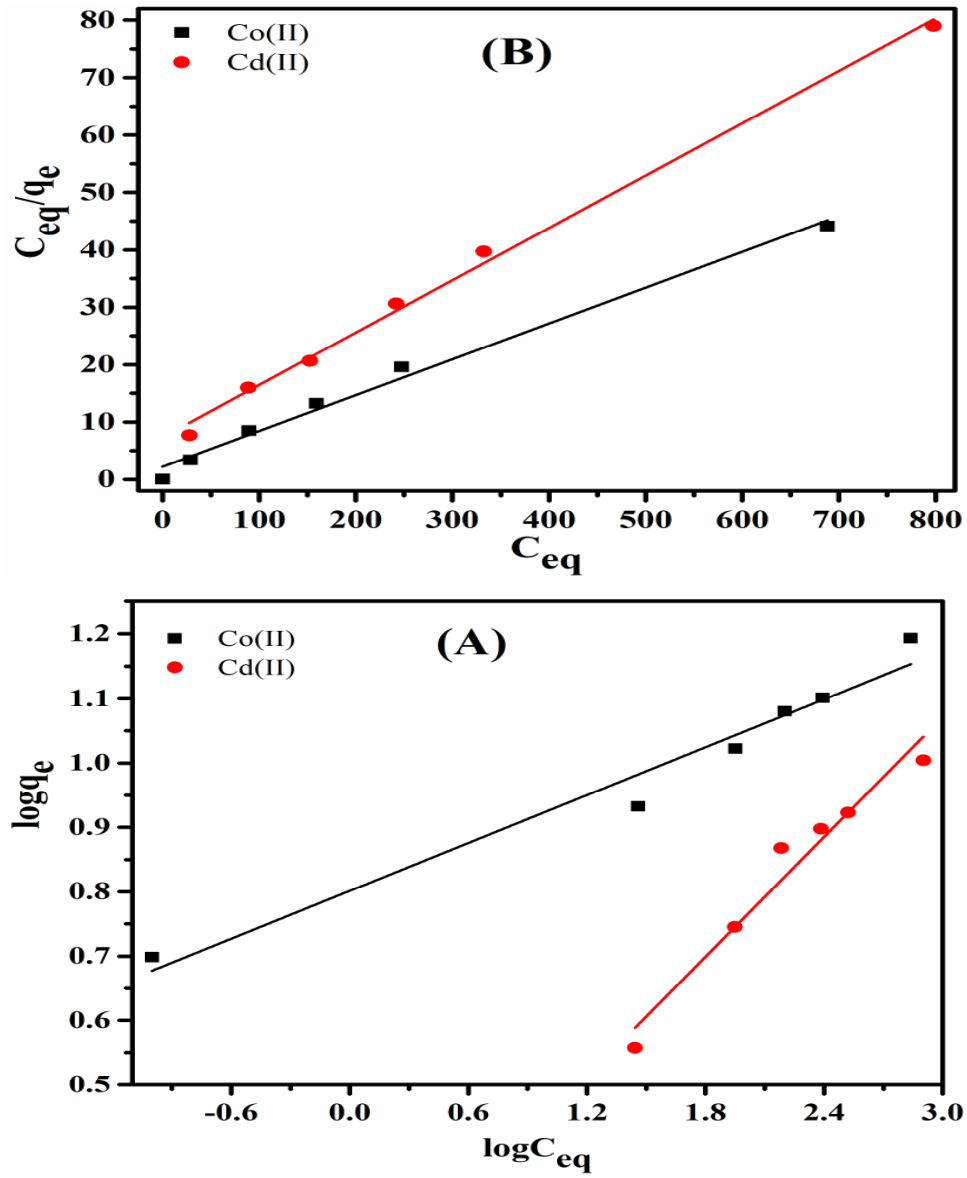
(B)
Co(II)
Cd(II)
$C_{eq}/q_e$
$C_{eq}$
0
10
20
30
40
50
60
70
80
0
100
200
300
400
500
600
700
800
(A)
Co(II)
Cd(II)
$\log q_e$
$\log C_{eq}$
0.5
0.6
0.7
0.8
0.9
1.0
1.1
1.2
-0.6
0.0
0.6
1.2
1.8
2.4
3.0

**Fig. 4.**

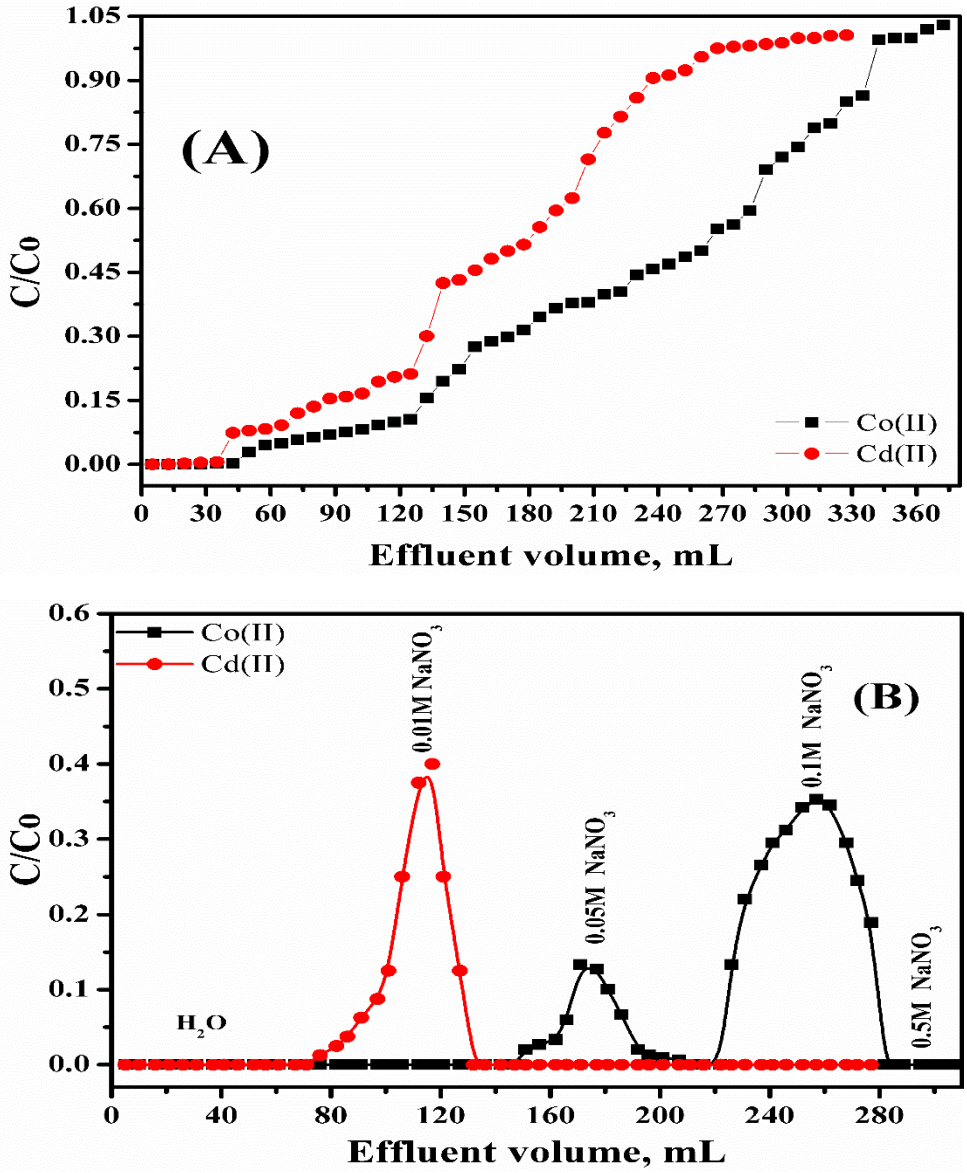
(A)
C/C0
Effluent volume, mL
Co(II)
Cd(II)
(B)
0.01M NaNO3
0.05M NaNO3
0.1M NaNO3
0.5M NaNO3
H2O

**Fig. 5.**